

2. ISEE International Joint Research Program 目次詳細

(所属・職名は2020年3月現在)
(Affiliation and Department displayed are current as of March 2020.)

(注1) : 新型コロナウイルスの影響で中止
(注2) : 新型コロナウイルスの影響で2020年度に延期し実施
(注3) : 新型コロナウイルスの影響で2020年度に延期し中止

研究代表者 Principal Investigator	所属機関 Affiliation	所属部局 Department	職名 Position	研究課題名 Project Title	頁 Page	備考 Remarks
David Tsiklauri	Queen Mary University of London	School of Physics and Astronomy	Senior Lecturer (tenured associate professor)	Investigation of the role of kink MHD waves in flare trigger model	58	
Stepan Poluianov	University of Oulu, Finland	Space Climate Research Unit and Sodankylä Geophysical Observatory	Postdoctoral researcher	Model of production-transport-deposition of cosmogenic isotopes over Antarctica with verification with experimental data		(注3)
Rangaiah Kariyappa	Indian Institute of Astrophysics, Koramangala, Bangalore 560034, INDIA	Solar & Space Physics Division	Former Professor & Chairman	UV & EUV Solar Irradiance Variability and their impacts on Earth's Climate & Space Weather	60	
Tulasiram Sudarsanam	Indian Institute of Geomagnetism	Space Weather and Upper Atmospheric Science	Associate Professor	Prompt penetration of convection/overshielding electric fields during the onset of substorms	66	
Baolin Tan	National Astronomical observatories of Chinese Academy of Sciences (NAOC)	solar physics	Professor	Testing diagnosing of the coronal magnetic field from solar radio observations	68	
Matthias Förster	GFZ German Research Centre for Geosciences	Section 1.1 (Space Geodesy)	senior scientist (retired)	Relation of Swarm satellite and SuperDARN ground-based ion drift measurements	70	
Iskhaq Iskandar	University of Sriwijaya	Physics	Professor	Variability in satellite-derived surface chlorophyll-a, Ekman transport and sea surface temperature in the Banda Sea	72	
Anukul Buranapratheprat	Burapha University	Department of Aquatic Science	Assistant Professor, Faculty of Science	Detection and modeling of green Noctiluca bloom in the Gulf of Thailand using satellite ocean color	74	
Mykola Gordovskyy	University of Manchester	School of Physics and Astronomy	Research Associate	Fluid-kinetic modelling of magnetic reconnection in solar flares and their impact on the heliosphere	76	(注2)
Viswanathan Lakshmi Narayanan	National Atmospheric Research Laboratory	Not Applicable	INSPIRE Faculty	Investigation of the relationship between nighttime electrified medium scale traveling ionospheric disturbances and middle latitude spread F	78	
Seth Claudepierre	The Aerospace Corporation	Space Sciences Department	Member of the Technical Staff	Collaborative radiation belt science: Using multi-spacecraft observations to further our understanding of wave-particle interactions in the Earth's magnetosphere		(注3)
Samuel Krucker	University of Applied Sciences Northwestern Switzerland	Institute for Data Science	Professor	The NoRH/RHESSI flare catalogue: statistical paper and planning for the future	80	
Kim Nielsen	Utah Valley University	Physics	Associate Professor	Energetics of Arctic Stratospheric and Mesospheric Coupling Due to small-scale gravity waves	82	
Pravata K. Mohanty	Tata Institute of Fundamental Research (TIFR)	Department of High Energy Physics	Fellow	Tomographic study of galactic cosmic anisotropy in near-Earth space by Multi-directional cosmic ray observations	84	
Ondrej Santolík	Institute of Atmospheric Physics	Department of Space Physics	Senior research scientist / Professor	Investigation of electromagnetic wave phenomena using multipoint measurements		(注3)

Hiroatsu Sato	German Aerospace Center (DLR)	Institute of Communications and Navigation	Research scientist	Imaging meter-scale density irregularities associated with midlatitude TIDs	86	
---------------	-------------------------------	--	--------------------	---	----	--

Investigation of the role of kink MHD waves in flare trigger model

PI David Tsiklauri (Queen Mary University of London)

ABSTRACT. The ability to predict the occurrence of solar flares in advance is important to humankind due to the potential damage they can cause to Earth's environment and infrastructure. It has been shown in Kusano et al. (2012) that a small-scale active region (AR) with its flux reversed relative to the potential component of the overlying field appearing near the polarity inversion line (PIL) is sufficient to effectively trigger a solar flare. In this study we perform further 3D magnetohydrodynamic simulations to study the effect that the motion of these small-scale AR on the effectiveness of flare triggering. The effect of two small-scale ARs colliding is also simulated. The results indicate that the strength of the triggered flare is dependent on how much of the overlying field is disrupted by the AR. Motion along the PIL can dramatically increase the strength of the flare increasing the peak Kinetic Energy (KE) more than threefold in the most extreme case simulated. Motion across the PIL or rotation of the AR however are seen to detract from the strength from the strength of the flare. Colliding AR also produce a much stronger flare as the flares triggered by each individual AR coalesce. These results show that significantly stronger flares can result from having multiple such AR or simply from the motion of such an AR along the PIL of a sheared overlying field.

The main findings of pioneering work by Kusano et al. (2012) were systematically surveying the nonlinear dynamics caused by a wide variety of magnetic structures in terms of three-dimensional magnetohydrodynamic simulations. As a result, they determined that two different types of small magnetic structures favor the onset of solar eruptions. These structures, which should appear near the magnetic PIL, include magnetic fluxes reversed to the potential component or the non-potential component of major field on the PIL. The central finding of Kusano et al. (2012) was their Fig. 2, where they considered maximum kinetic energy achieved during a solar eruption as a function of shear angle θ_0 and the injected small-scale field azimuthal orientation ϕ_e . It was found that large values of θ_0 close to 90° and $\phi_e = 180^\circ$ produces the most favorable conditions for the solar flares. In this work we consider the most favorable condition for the solar flares as in Kusano et al. (2012), but now in addition we impose linearly polarized oscillation on the emerging small-scale AR. We study the effect of amplitude and frequency variation of linearly polarized oscillations of single, emerging ARs and collision of two emerging ARs on solar flare efficiency. Our motivation is two-fold:

(i) We would like to investigate how oscillations in the AR, both linear and torsional, might affect the previous results of Kusano et al. (2012). Such oscillations can come from a Alfvén waves travelling along the emerging magnetic flux tube that extends from solar corona down to below photosphere.

(ii) Sunspots are known to collide/coalesce. Hence we would like to study how this affects the amount of energy released during the flare modelled by emerging and at the same time colliding, small-scale fields interacting with an overlaying, pre-existing field with $\theta_0 = 80^\circ$ and $\phi_e = 180^\circ$ configuration.

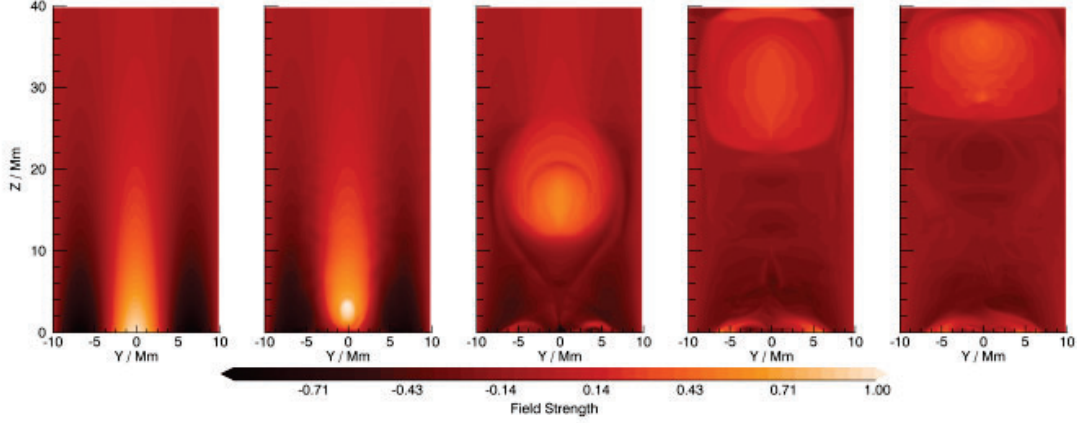


Figure 1. Contour plots of B_z through the plane $x = 0$ at times 0, 5, 10, 15 and $20 \tau_A$ for the simulation in which $A_x = 4$ Mm, $f = 1.0 \tau_A^{-1}$ showing clearly the magnetic reconnection and subsequent CME formation.

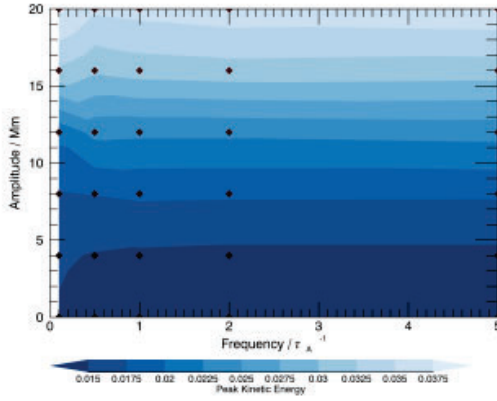


Figure 2. A contour plot of the peak kinetic energy for different values of amplitude A_x and frequency f with amplitude A_y fixed at 4 Mm.

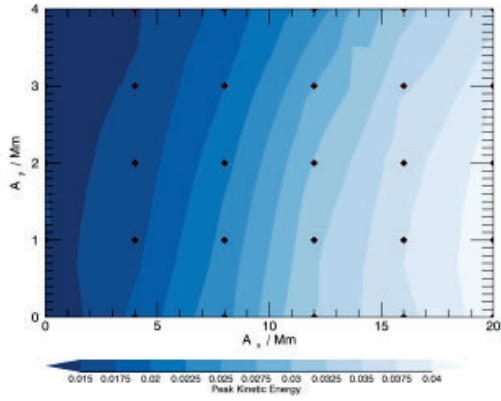


Figure 3. A contour plot of the peak kinetic energy for different values of amplitudes A_x and A_y with frequency fixed at $f = 1 \tau_A^{-1}$.

We find that movement of the small-scale AR along the PIL increases the strength of the flare triggered whilst movement of the AR away from the PIL decreases the flare strength, as illustrated in above figures. Torsional motion seems to have little effect on the flares although sustained rotation that moves the AR too far from its most favourable orientation (180° relative to the PIL) does reduce the strength of the flare. Finally collisions lead to more energetic flares due to both the movement of the individual AR and the coalescence of the flares triggered by each emerging AR.

periods of stay in ISEE

C. Boocock, 6-24 May, 2019; D. Tsiklauri, 17-24 August, 2019

list of publications

C. Boocock, K. Kusano, and D. Tsiklauri, “The Effects of Oscillations and Collisions of Emerging Active Regions on the Triggering of Solar Flares” Submitted to ApJ

Conferences: results will be presented at the next UK Roy. Astron Soc. National Astronomy meeting 2020

Project Title: *EUV, UV & X-ray Solar Irradiance Variability and their Impacts on Earth's Climate & Space Weather*

Principal Investigator Name (Affiliation)

Dr. R. Kariyappa

Former Professor, Indian Institute of Astrophysics

Bangalore 560034, India

This research work was carried out in collaboration with Shinsuke Imada (ISEE/Nagoya University), Kanya Kusano (ISEE/ Nagoya University), H.N. Adithya (PhD student, YIESPL/IIA), Joe Zender (ESA/ESTEC), L. Dame (CNRS/LATMOS), G. Giono (KTH), Mark Weber (CFA/Harvard), and E.E. DeLuca (CFA/Harvard).

This project was supported by ISEE/Nagoya University under ISEE International Joint Research Program. My period of stay in ISEE was from 16 June to 18 July 2019. I appreciate the generous support and hospitality that I received during this period, and the warm disposition of staff and students I worked and stayed at ISEE. Particularly I am very thankful to Dr. Kanya Kusano (Director) and Dr. Shinsuke Imada for their constant support and for a productive discussion which lead to many interesting and important results.

Project Summary:

The Sun is the primary source of energy responsible for governing both the weather and climate of Earth. For that reason alone, one would expect that changes in the amount and type of energy Earth received from the Sun could alter weather and climate on the Earth. The variations in the EUV, UV & X-ray irradiance are produced by surface manifestation of solar magnetic activity. Considering the variations in the solar EUV, UV & X-ray flux may cause significant changes in the Earths climate, understanding the physical origin of EUV, UV & X-ray irradiance changes is an extremely important issue in Solar and Space Physics and in Solar Terrestrial Physics.

Recently we have worked on PROBA2/SWAP & SDO/AIA spatially resolved full-disk images to understand the EUV & UV solar irradiance variability measured using PROBA2/LYRA instrument and published a large number of research papers. During my visit to ISEE under this program, we had a long discussion on Solar X-ray irradiance and decided to work on Hinode/XRT full-disk spatially resolved soft X-ray images to understand total solar X-ray flux variations measured by GOES (1-8 Å). For the first time we have analysed the XRT full-disk X-ray images to segment the different coronal features. We have developed an algorithm in Python to analyse the XRT images for the period from 2007 to 2012 in two filters namely, Al mesh and Ti poly and segmented automatically the different coronal features such as

Active Regions (ARs), Coronal Holes (CHs), Background (BGs) and X-ray Bright Points (XBPs). We have estimated the total intensity of all these features and of the full-disk and compared with total solar X-ray flux measured in 1-8 Å from GOES instrument and with solar cycle. It is found that all the coronal soft X-ray features are well correlated with GOES X-ray flux variations and with the sunspot numbers. We found that the active regions are more responsible for solar X-ray irradiance variations compared to other features. In addition the number of XBPs appears to be anti-correlated with the solar activity, but need to be confirmed with further studies. The time series of all the features will contribute to total solar X-ray irradiance variability and shown that the variations in integrated solar X-ray flux (GOES 1-8Å) can be explained by spatially resolved and segmented full-disk soft X-ray images (Hinode/XRT).

Scientific Background:

Since the radiative output of the Sun is one of the main driving forces of the terrestrial atmosphere and climate system, the study of solar energy raises is of increasing interest. Although the long-term change in total solar irradiance (the solar energy flux integrated over the entire spectrum) is considered to be one of the major natural forces of the Earth's climate system, the study of extreme ultraviolet (EUV) and ultraviolet (UV) and X-ray irradiance variability is equally important in solar physics and in solar terrestrial atmosphere. Indeed, EUV irradiance is the main energy input for the Earth's upper atmosphere with important effects on the ionosphere and thermosphere. The solar EUV and UV & X-ray fluxes thus play a major role in Solar-Terrestrial relationships. Understanding their variability is thus an important issue for space weather and climate applications. Understanding the EUV and UV & X-ray irradiance variability from spatially resolved intensity and magnetic field observations of the Sun from Space and Ground based Missions is an important issue in space weather and climate applications.

In the recent years we made a detailed studies to understand the EUV & UV solar irradiance from spatially resolved full-disk intensity and magnetic field images observed by PROBA2/SWAP, SDO/AIA

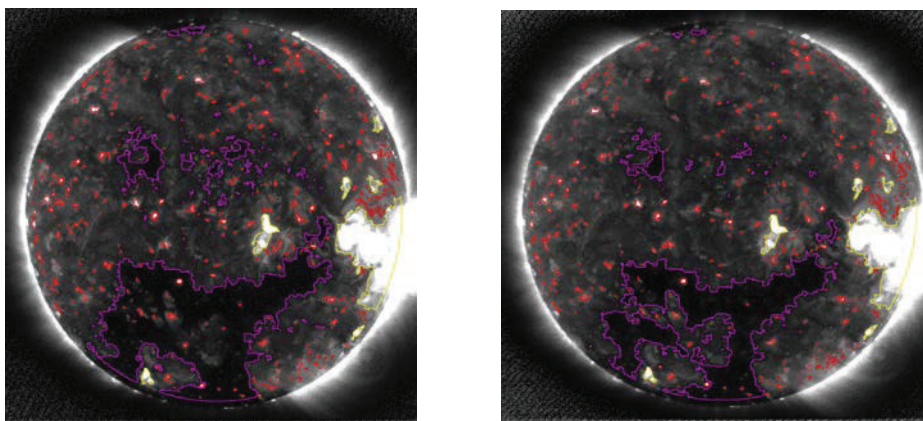


Figure 1: Segmented solar X-ray images obtained with Hinode/XRT in Ti poly (left image) and Al mesh (right image) filters on 13-01-2008

and SDO/HMI instruments. We determined the contribution of the different features and the role of

magnetic field to EUV & UV irradiance variability. In the present project we proposed to use Hinode/XRT full disk X-ray images for the period from 2007 to 2012 and segregate the different features (such as active regions, coronal holes, background and x-ray bright points) of the solar corona. Finally and combinedly to determine the role of UV, EUV & X-ray irradiance variations on Earth's Climate & Space Weather.

Observational Data and Image analysis:

We have used full-disk spatially resolved X-ray images for the period 2007 - 2012 observed by Hinode/XRT instrument simultaneously in two filters: Ti poly and Al mesh filters. A segmentation algorithm has been developed in Python to segment automatically the different coronal features (such as active regions - ARs, coronal holes - CHs, background regions - BG and X-ray bright points - XBPs) based on intensity criteria and their morphology and sizes of the features. We derived the total intensity of all the segmented features for the entire period and estimated their contributions to total full-disk intensity and to total solar X-ray flux measured in 1-8 Å using GOES.

The preliminary results of these analysis are presented in this report.

Preliminary Results:

For the first time the full-disk soft X-ray images obtained from Hinode/XRT have been analysed & compared with GOES (1-8Å) total X-ray irradiance. We have segmented the different coronal X-ray magnetic features (ARs, BGs, XBPs & CHs) to understand their intensity variations. We derived the total intensity of individual features and the full disk intensity values in the two filters (Ti poly & Al mesh). We found that all the features show intensity variations as a function of solar magnetic cycle (sunspot numbers). In addition to intensity values of all the features, we have identified and counted automatically the X-ray bright points over the entire disk for the whole period from 2007 to 2012. We found that there is an indication of anti-correlation of total number of XBPs with solar cycle, need to be confirmed with detailed studies.

Variations in the quantities resulting from the segmentation, namely the integrated intensity of ARs/CHs/QS/FD regions, are compared with the GOES 1-8Å Solar X-ray irradiance variations. We found that the X-ray full-disk intensity over ARs/CHs/QS/FD is well correlated with the GOES Solar X-ray (1-8 Å) irradiance variations. We observed that all the coronal features will contribute significantly to total solar X-ray irradiance. We noticed that sophisticated feature identification and segmentation tools are important in providing more insights into the role of various coronal features in both the short- and long-term changes in the solar X-ray irradiance. The spatially resolved and segmented full-disk X-ray images (XRT) will help to explain fully the total solar X-ray flux variations, measured Sun as a Star (by GOES).

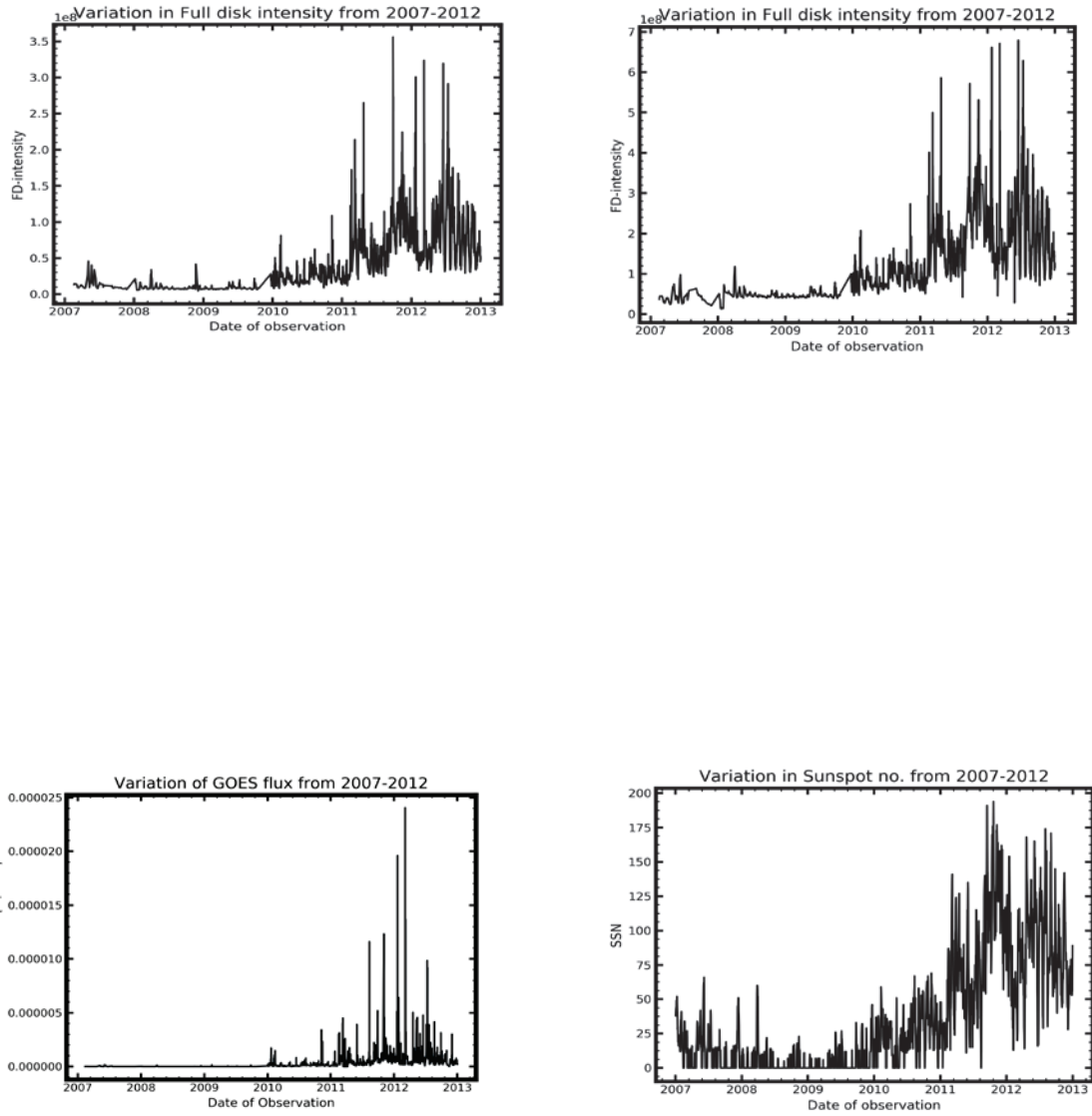


Figure 2: Variation of total intensity of the full-disk solar X-ray image observed in Ti poly (top left) & Al mesh (top right) filters, GOES (1-8 Å) total solar X-ray flux (bottom left panel) and for comparison Sunspot Numbers (bottom right panel) for the period: 2007 to 2012.

Importance of this project and Future Work:

The importance of this project is to understand the physical mechanism of the variability of solar EUV, UV & X-ray irradiance, segment the various features, the contribution of different magnetic features, and to determine the impacts of EUV, UV & X-ray irradiance on Earth's Climate and Space Weather. Particularly the Hinode/XRT full-disk images have not been used earlier to study the solar X-ray irradiance variability. So it is important to use them to explain the solar X-ray flux variability. This research effort will lead to the PhD thesis work of Mr. H.N. Adithya.

(i) Since we have observations at least in two filters (Ti poly and Al mesh) simultaneously and their

corresponding temperature response curves, we plan to derive the temperature of different coronal features and for the full-disk and to study the temperature variations associated with the features and finally to derive the temperature maps of the full solar corona;

(ii) We plan to compare the full-disk segmented intensity images with SDO/HMI full-disk magnetograms to determine the magnetic field of all the features;

(iii) This research effort will help to determine the role of magnetic field in the solar X-ray irradiance variability, similar to the work done recently by us on the role magnetic field in EUV & UV irradiance variations;

(iv) Construction of intensity field, magnetic field and temperature maps of the full-disk solar corona;

(v) Estimation of the impacts of EUV, UV & X-ray irradiance on Earth's Climate and space weather;

(vi) This research effort will be a part of the PhD thesis of Mr. H.N. Adithya.

Seminar:

I gave a seminar on "Coronal & Photospheric Magnetic Features from Spatially Resolved Images to Understand EUV & UV Solar Irradiance Variability & their impacts on Earth's Climate and Space Weather" on June 26, 2019 at ISEE.

Visited NAOJ:

I visited National Astronomical Observatory of Japan (NAOJ), Mitaka from June 30 to July 04, 2019 on the invitation of Dr. Tetsuya Watanabe for a scientific discussion with the faculty members of Solar Physics Division on solar X-ray irradiance, and given a seminar on EUV & UV Solar Irradiance.

Papers presented at the International Conferences/Symposium/Meetings:

(i) Adithya, H.N., Kariyappa, R., Shinsuke, Imada, Kanya Kusano, Zender, J.J., Dame, L., Giono, G., Mark Weber, and Deluca, E.E., "Solar X-ray Irradiance Variability & its Impacts on Earth's Climate & Space Weather - Preliminary Results, presented at the PSTEP4/2ISEE International Symposium held on January 28 - 30, 2019, ISEE/Nagoya University, Nagoya, Japan - presented by R. Kariyappa.

(ii) Adithya, H.N., Kariyappa, R., Shinsuke, Imada, Kanya Kusano, Zender, J.J., Dame, L., Giono, G., Mark Weber, and Deluca, E.E., Solar X-ray Irradiance Variability from Spatially Resolved Full-Disk Images from Hinode/XRT, presented at 5th Asia Pacific Solar Physics, February 3-7, 2020, Pune, India - presented by H. N. Adithya.

Publications - in progress:

(i) Adithya, H.N., Kariyappa, R., Shinsuke, Imada, Kanya Kusano, Zender, J.J., Dame, L., Giono, G., Mark Weber, and Deluca, E.E.: 2020, Contribution of Coronal Magnetic Features to Total Solar X-ray Irradiance Variability, in preparation.

(ii) van der Zwaard, R., Bergmann, M., Zender, J.J., Kariyappa, R., Giono, G. and Dame, L.: 2020, Segmentation of coronal features to understand the solar EUV and UV irradiance variability III. Inclusion and Analysis of Bright points, A&A, under review.

(iii) Giono, G., Zender, J.J., Kariyappa, R., and Dame, L.: 2020, Understanding the long-term

periodicities seen in the EUV/UV solar irradiance, Daily segmentation of EUV/UV images over a 7-years period to investigate irradiance periodicities from days to month, To be Submitted to A&A.

Project Title: Prompt penetration of convection/overshielding electric fields during the onset of substorms

Tulasiram Sudarsanam
Associate Professor
Indian Institute of Geomagnetism, India

Purpose

The main purpose of this project work is to investigate the Prompt Penetration Electric Fields during the onset of substorms and its impact on the equatorial and low-latitude ionosphere. Further, it is also proposed to investigate the MLT dependence on the eastward/westward polarity of PPEF during the substorms.

Method

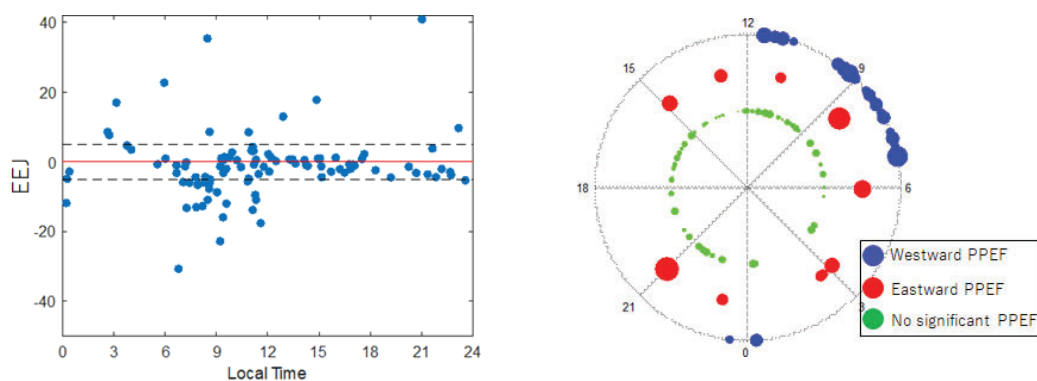
A multi-observational approach is adopted in this investigation. The ground based magnetometer observations from Indian, Japanese and Brazilian sectors have been analyzed to study the equatorial electrojet variations during the onset of substorms. A novel selection criteria have been defined to automatically detect the onset of isolated substorms from long term observations of Wp-index, AU/AL indices using a computer program. The substorm selection criteria includes (i) A sharp increase in Wp-index (magnitude ≥ 0.4 nT @ ≥ 0.05 nT/min) from a quiescent pre-epoch state (standard deviation of previous 30 min ≤ 0.1 nT), (ii) A simultaneous decrease in AL (magnitude ≤ -500 nT), (iii) The background solar wind conditions must be steady i.e., peak-to-peak changes in IEFy ≤ 2.5 mV/m and standard deviation of dynamic pressure must be less than 1 nPa over the 45 minutes centered on the time of substorm onset. The criterion (i) and (ii) detects the onset of a substorm while criterion (iii) ensures the steady background SW conditions. Hence, the observed changes in the EEJ can be chiefly considered as PPEFs in response to the onset of substorms. Further, the SuperDARN HF radar and ground based GPS-TEC observations have also been considered to investigate the low-latitude ionospheric response to the PPEFs induced due to the onset of substorms. Both the case study and the statistical investigations have been made. Salient results are briefly summarized hereunder.

Summary of results

The strong substorm event occurred around 1730 UT under steady southward IMF Bz conditions during the St. Patrick's day storm on 17th March 2015 has been investigated to study the PPEF effects at low-latitudes. The equatorial electrojet (EEJ) exhibited a substantial increase indicating strong eastward PPEF with the onset of substorm. Further, enhanced westward electrojet currents have also been observed on the night side (Japanese sector). The strong eastward PPEF during this event has caused the equatorial super fountain and rapid redistribution of low-latitude plasma into symmetric EIA crests within 15 minutes over the Brazilian sector. The high latitude convection maps from SuperDARN observations indicates that the reconfiguration of convection cells in the southern high latitudes during this event and the resultant enhancement of convection electric field led to this eastward (westward) PPEF on day (night) side [Tulasi Ram et al., 2019].

A statistical study is further carried out to investigate the polarity of PPEF during the onset of isolated

substorms and its local time dependency using long term EEJ observations (2001-2012) from the Indian sector and Wp index measurements from ISEE. A total 102 isolated substorms detected using a computer program based on the above selection criteria have been analyzed to investigate the EEJ response and its MLT dependency. While most of the isolated substorms (68 cases) do not cause significant disturbances in the EEJ (≤ 5 nT), about 10 cases caused eastward EEJ disturbance (> 5 nT) while the other 24 substorms have caused westward EEJ disturbance (< -5 nT). The below figures show the local distribution of EEJ disturbances. It can be seen from these figures that the westward EEJ disturbances are mostly confined to morning sector i.e., 06 – 12 LT. However, the eastward EEJ disturbances, though only 10 cases, do not exhibit any local time preferences. Further investigation on the factors responsible for the dawn-to-noon sector preference of westward EEJ response is currently underway



Visit to ISEE

The PI, Dr. S. Tulasiram has visited Nagoya University during the period from 23rd Dec 2019 – 07th Feb 2020 and conducted the above joint research investigations along with the host professor Prof. K. Shiokawa and his group at ISEE, Nagoya University under ISEE international joint research program – 2019. Additional collaborative investigations are also carried out on the solar wind density control on the PPEF and Dilatory and downward development of shorter scale irregularities in the plasma bubbles during the this visit.

List of Publications

- S. Tulasi Ram, B. Nilam, N. Balan, Q. Zhang, K. Shiokawa, D. Chakrabarty, Z. Xing, K. Venkatesh, B. Veenadhari and A. Yoshikawa, Three different episodes of prompt equatorial electric field perturbations under steady southward IMF Bz during St. Patrick's day storm, *J. Geophys. Res. Space Physics*, 124, <https://doi.org/10.1029/2019JA027069>, 2019.
- S. Tulasi Ram, B. Nilam, K. Shiokawa, M. Nose, The prompt penetration electric fields during the onset of isolated substorms, *J. Geophys. Res.*, 2020 (under preparation).
- B. Nilam, S. Tulasi Ram, K. Shiokawa, N. Balan and Q. Zhang, The solar wind density control on the Prompt Penetration electric Field and Equatorial Electrojet, *J. Geophys. Res.*, 2020 (under review).
- S. Tulasi Ram, K. K. Ajith, T. Yokoyama, M. Yamamoto, K. Hozumi, K. Shiokawa, Y. Otsuka and G. Li, Dilatory and downward development of 3-meter scale irregularities in the Funnel-like region of a rapidly rising Equatorial Plasma Bubble, *Geophys. Res. Lett.*, 2020 (under review).

Project Title: Testing diagnosing of the coronal magnetic field from solar radio observations

Baolin Tan

(National Astronomical Observatories of Chinese Academy of Sciences)

Under the support of this joint project, we use the multi-wavelengths observations, including radio observations of MUSER, NoRH, and IPRT/AMATRAS, and EUV imaging observations of AIA/SDO to diagnose the nonthermal processes and precursors of solar flares and investigate the related energy release and particle acceleration. We published 3 collaborative papers in ApJ, and our results are in following:

- (1) We demonstrated 3 types of solar fast-drifting radio bursts (FDRBs), including type III pair bursts, narrowband stochastic spike bursts, and spike-like bursts. Although all of them have fast frequency-drifting rates, but they are intrinsically different from each other in frequency bandwidth, drifting rate, and statistical distribution which are possibly generated from different accelerating mechanisms. The type III pair bursts may be triggered by high-energy electron beams accelerated by the flaring magnetic reconnection, spike bursts are produced by the energetic electrons accelerated by a termination shock wave triggered by the fast reconnecting plasma outflows impacting the flaring loop top, and the spike-like bursts are possibly generated by nonthermal electrons accelerated by moving magnetic reconnection triggered by interaction between CME and the background magnetic fields.
- (2) We study a solar eruptive prominence associated to a flare/CME event by microwave and EUV observations. The evolution can be divided into three phases: slow rise, fast expansion, and ejection. In the slow-rise phase, the prominence continuously twists with a patch of bright emission appearing around the top. When one leg interacts with the local small-size loops, the fast expansion is initiated and the flare takes place. The prominence grows rapidly accompanying with a series of localized bright points. These localized bright structures, first appearing at the top and then scattering in the entire prominence structure, are co-spatial with EUV bright threads, fibers, or spots in both high- and low-temperature passbands. They display significant temporal variations on the scale of 3-5 s in the microwave observations. This behavior could be interpreted in the frame of the small-scale and short-term process of energy releases in the twisted magnetic structure.
- (3) From the analysis of radio images observed by MUSER at frequencies of 1.2-2.0 GHz for the first time, microwave images by the NoRH, UV and EUV images by AIA/SDO, and a magnetogram by HMI/SDO, we found three different QPPs in a solar flare: UV-QPPs with a period of ~ 4 min at 1600 Å images near the center of the active region lasting from the preflare phase to the impulsive phase; EUV-QPPs with a period of about 3 min along the

circular ribbon during the preflare phase; and radio QPPs with a period of about 2 min at frequencies of 1.2-2.0 GHz around the flaring source region during the impulsive phase. We suggest that the 4 min UV-QPPs should be modulated by the sunspot oscillations, and the 3 min EUV-QPPs are closely related to the 2 min radio-QPPs for their source regions connected by a group of coronal loops. We propose that the intermittent magnetic reconnecting downward and upward plasmoids may be the possible trigger of both the preflare 3 min EUV-QPPs and the impulsive 2 min radio-QPPs. The possible mechanism is LRC-oscillation, which is associated with the current-carrying coronal loops, and the existence of preflare QPPs may be a possible precursor to solar flares.

Periods of stay in ISEE: Prof Baolin Tan and Dr. Chengming Tan visited and stayed in ISEE from 2019 October 25 till November 6.

List of publication:

- (1) Tan B.L., Chen Nai-hwa, Yang Ya-hui, Tan C.M., Masuda S., Chen X.Y., Misawa H., Solar Fast Drifting Radio Bursts in an X1.3 Flare on 2014 April 25, 2019, ApJ, 885:90
- (2) Chen X.Y., Yan Y.H., Tan B.L., Huang J., Wang W., Chen L.J., Zhang Y., Tan C.M., Liu D.H., Masuda S., Quasi-periodic pulsations before and during a solar flare in AR 12242, ApJ, 2019, 878, 78
- (3) Huang J., Tan B.L., Masuda S., Cheng X., Susanta B., and Melnikov V.F., The localized microwave and EUV bright structures in the eruptive prominence, 2019, ApJ, 874, 176

We also presented several reports in international scientific conferences:

- (1) Tan Baolin, Solar radio spectral fine structures and diagnostics of non-thermal processes (Oral presentation), CESRA2019, Potsdam, Germany, 2019 July 8-13
- (2) Tan Baolin, Radio Precursor of Solar Flares (Oral presentation), ISEE seminar, Nagoya University, Japan, 2019 October 30
- (3) Tan Baolin, Introduction of Solar Radio Research in NAOC (Oral presentation), ISEE Seminar, Nagoya University, Japan, 2019 October 29.
- (4) Tan, Baolin, Radio Precursors of Solar Flares (Oral presentation), Russian conference of solar physics in 2019, Saint Petersburg, Russia, 2019, October 9

Project Title

Relation of Swarm satellite and SuperDARN ground-based ion drift measurements

Matthias Förster

GFZ German Research Centre for Geosciences,
Section 1.1, Telegrafenberg, 14473 Potsdam, Germany

Purpose:

Our study aimed on comparisons of Swarm satellite and SuperDARN ground-based ion drift measurements, focusing on the Japanese radar facilities of the SuperDARN network, Hokkaido East ("hok") and West ("hkw"). We planned both statistical analyses of the ion drift behavior and some closer investigations of selected periods in the sense of individual case studies of geomagnetic storm periods. It was intended, that the synoptic view of satellite and ground-based observations provides some clues for a better understanding of the relation between larger- and smaller-scale ion drift structures and the physical coupling processes within the complex M-I-T system.

Methods:

The Swarm satellites on their near-polar orbits are equipped with two Thermal Ion Imager (TII) sensor heads at the front side of the satellites. The analyses of the ion images on the CCD cameras allow in principle a 3-D vector record of the ion drift with the vertical and horizontal cross-track components from the respective sensor heads and the along-track component from both sensors independently. It appeared however, that due to various problems with the sensor heads (contamination by water vapor) and charging effects in the near-spacecraft environment, it was useful to develop first a simplified data set with the cross-track ion drift component only. The initial release (version 0101) of the data set dates from November 2016, an improved, better calibrated version 0202 was issued just during my second stay at ISEE in February 2020. We used the horizontal cross-track component of the TII sensors which is almost aligned with SuperDARN line-of-sight drift measurements for comparisons during overflights. For the data extraction and visualization we used the SPEDAS software, provided from ISEE.

Results:

The task of direct comparisons of ion drift components of the cross-track TII on the one hand side and of the l.-o.-s. SuperDARN observations on the other necessitated some IDL software development of reading and mapping the data accordingly. The 2-Hz TII level-1b satellite data are given as daily cdf-files; the SuperDARN drift values were deduced using the SPEDAS software package. It appears, that the in-situ satellite drift component measurements have generally larger magnitudes, sometimes considerable by more than factor 2. This was already shown in previous studies (e.g., Koustov et al., 2019, doi: 10.1029/2018JA026245), and seems to be valid also for the latest data issue (version 0201). A systematic, comprehensive statistical study could not be done during the relatively short run time of this project. This has to be postponed to a later stage of continuing cooperation, providing an even better calibration and improved data interpretation of the TII drift measurements will be available then. Minor structures as, e.g., the subauroral polarization streams (SAPS) could be identified and compared without doubt and were used for a few event studies like the one in the publication.

Periods of stay in ISEE:

- 1.) 30 June – 05 July 2019
- 2.) 16-26 February 2020

Publications:

- 1.) Astafyeva, E., Bagiya, M. S., Förster, M., & Nishitani, N. (2020). “Unprecedented Hemispheric Asymmetries During a Surprise Ionospheric Storm: A Game of Drivers”. *Journal of Geophysical Research: Space Physics*, **125**, e2019JA027261. <https://doi.org/10.1029/2019JA027261>.

Presentations:

- 1.) “Interhemispheric differences of the high-latitude ionospheric convection deduced from Cluster EDI drift measurements”, M. Förster and S. Haaland, Workshop on Pulsating Auroras, July 2-3, 2019, ISEE, Nagoya.
- 2.) “Symmetries and asymmetries of the Earth’s magnetic field and their implications for the magnetosphere-ionosphere-thermosphere (M-I-T) coupling”, M. Förster, 61st Colloquium at the ISEE, February 20, 2020.

Variability in satellite-derived surface chlorophyll-a, Ekman transport and sea surface temperature in the Banda Sea

Iskhaq Iskandar
University of Sriwijaya, Indonesia

Background

The Banda Sea, bordered by the Southern Molucca islands (i.e. Seram, Sula and Buru Islands) on the north and Nusa Tenggara Islands Chain on the south, Sulawesi Island on the west and Papua Island on the east, is located on the route of Indonesian Throughflow (ITF). The ITF transports water masses into the Banda Sea through the Makassar Strait/Flores Sea in the west and the Molucca Strait on the North with major transport is coming from the Makassar Strait (Gordon and Fine, 1996). There two outflow channels of ITF from the Banda Sea, namely the Ombai Strait and the Timor Passage. The ITF plays an important role on the global ocean and climate circulation (Lee et al., 2002) and ecosystem dynamics (Iskandar et al., 2010). Using coupled bio-physical model, Iskandar et al. (2010) demonstrated that the ITF provides nutrient reach-water that sustained surface chlorophyll-a bloom in the southern Java during the positive Indian Ocean Dipole (IOD).

Purpose

This study is designed to evaluate the seasonal and interannual variation of physical and biological ocean parameters in the ITF region, in particular in the Banda Sea and its surrounding seas.

Data and Methods

The chl-a concentration data were obtained from the Moderate Resolution Imaging Spectroradiometer (MODIS) on board of the Terra and Aqua satellites. Monthly data at 9 km spatial resolution from January 2003 until December 2015 were downloaded from the Ocean Colour web site (<http://globcolour.info>).

The SST dataset were derived from the daily Optimum Interpolation Sea Surface Temperature (OI-SST) of the NOAA. The data cover a period of January 2003 to December 2015. Monthly averages were calculated from these daily fields. The spatial resolution of the SST data is $0.25^{\circ} \times 0.25^{\circ}$. In order to evaluate the dynamical forcing underlying surface chl-a variation in this area, surface wind data obtained from the ECMWF ERA5 reanalysis were used to calculate the Ekman transport. The data cover a period from January 2003 to December 2015 having horizontal resolution of 0.25° .

We examine their temporal means and seasonal cycles. We, then, removed the seasonal cycles to analyze at the nonseasonal variability. The nonseasonal variability is, in turn, divided into interannual and intra-annual timescales.

Results

Our analysis on the spatial temporal variability of physical and biological ocean parameters in the Banda Sea is still in progress. However, during our analysis, we found another interesting

result from the western part of the ITF, namely in the Karimata Strait, which connects the South China Sea and the internal Indonesian seas through the Java Sea.

Monthly climatological fields of the surface chl-a in the Karimata Strait during the northwest monsoon (December – March) until the spring monsoon-break (April – May) are presented in Figure 1 (*left*). Interestingly, the observed high chl-a concentration in the Karimata Strait during the northwest monsoon shows opposite situation with that observed along the western coast of Sumatra and along the southern coast of Java, which shows a low chl-a concentration during this season. It may suggest different mechanism underlying the chl-a bloom in the Karimata Strait. This high chl-a concentration during the northwest monsoon season could not be explained solely by the wind dynamics. As previously suggested, the enhancement of surface chl-a within the Indonesian seas (e.g. the Karimata Strait, the Java Sea and the Banda Sea) during the northwest monsoon season could be related to the increased of precipitation thus river discharge into the coastal region. High precipitation was observed (mainly over the land) from December until April (Figure 1, *right*). In particular, the highest precipitation was observed over the Sumatera in December and January co-occurred with the observed high chl-a concentration in the Karimata Strait. We hypothesize that the increase of precipitation may cause an increase of allochthonous nutrient from the land through the several river discharges in the eastern coast of Sumatra.

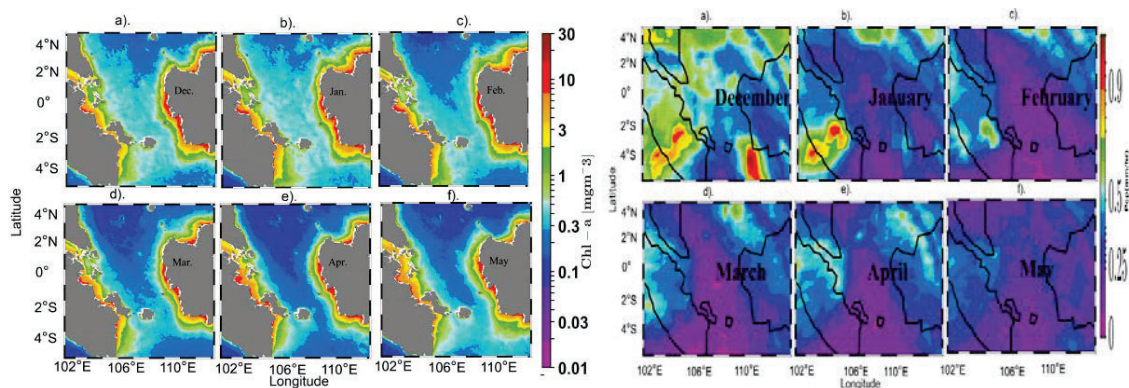


Figure 1. Monthly climatology of surface chl-a (*left*; mg/m^3) and precipitation (*right*; mm/hr) in the Karimata Strait during the northwest monsoon season (December – March) until the spring monsoon-break (April – May).

Period of stay in ISEE

1. Qurnia Wulan Sari : 5 – 14 November, 2019
2. Iskhaq Iskandar : 2 – 8 February, 2020.

List of Publication

Based on this study, we are still working to finalize a manuscript:

Seasonal and Interannual Variations of Surface Chlorophyll-a Variations in the Karimata Strait (to be submitted to IEEE Journal of Selected Topic in Applied Earth Observations and Remote Sensing)

Authors: Iskhaq Iskandar, Qurnia W. Sari, Eko Siswanto and Joji Ishizaka

Detection and modeling of green *Noctiluca* bloom in the Gulf of Thailand using satellite ocean color

Anukul Buranapratheprat (Burapha University)

Background

Harmful algal blooms (HABs) in the upper Gulf of Thailand (UGoT) are frequently caused by green *Noctiluca scintillans*, a dinoflagellate containing a symbiotic green alga named *Pedinomonas noctilucae*. The intensive bloom potentially causes massive fish mortality due to rapidly reducing oxygen in the water column and causes tourist disruption due to dirty seawater and foul odor. In this study, the differences in the apparent colors and pigment composition between green *Noctiluca* and other HABs (e.g., *Ceratium furca* and diatoms) are used to develop an algorithm for identifying the green *Noctiluca* bloom using ocean color remote sensing techniques and studied on its variability.

Purposes

1. To develop an algorithm to identify green *Noctiluca* blooms based on satellite ocean color data,
2. To investigate its variability in the relationship with the dynamical processes.

Methods

In situ bio-optical data and phytoplankton pigment compositions collected at the sea surface in wet and dry seasons between 2017 and 2018 were used to develop the algorithm. Phytoplankton community composition was estimated by the CHEMTAX program based on HPLC phytoplankton pigments. Each *in situ* remote sensing reflectance (R_{rs}) spectrum (320 nm – 950 nm) is identified as the blooming type by comparing it with the percentage of phytoplankton composition of the same survey station. The identified R_{rs} was normalized by R_{rs547} to reveal the specific spectral characteristics of plankton groups. A cluster analysis was performed to classify the normalized R_{rs} into related phytoplankton groups.

The HABs algorithm was applied to satellite data to identify the location of green *Noctiluca* blooms. The satellite R_{rs} was verified with *in situ* R_{rs} to assess accuracy. The blooming area was then validated with the reported HABs occurrence in UGoT. The satellite green-*Noctiluca* bloom images were then compared with the simulated surface circulation using Princeton Ocean Model (POM) to explain the variability of green *Noctiluca* blooming in the same period.

Results

Eight classes of phytoplankton were derived by HPLC-CHEMTAX (i.e., dinoflagellates, cryptophytes, prymnesiophytes, chrysophytes, chlorophytes in exponential stage, chlorophytes in stationary stage, cyanobacteria, and diatoms (Figure 1a). Green *Noctiluca* was classified in chlorophytes_1 (exponential phase) and chlorophytes_2 (stationary phase). The phytoplankton composition of each survey station comparing to *in situ* R_{rs} (Figure 1b) and the R_{rs547} normalized R_{rs} (Figure 1c) could classify the R_{rs} data into five groups, including 1) green *Noctiluca* blooms, 2) *Ceratium furca* blooms, and 3) diatoms blooms, and 4) mixed species, and 5) non-bloom waters.

We firstly focused on the MODIS wavelengths. Using cluster analysis of the normalized R_{rs547} and R_{rs667} showed five clusters of water types (Figure 1d). The cluster of green *Noctiluca* blooms was within 0.5 of the both normalized R_{rs} . The one of *C. furca* was within 0.5 of the normalized R_{rs488}

and over 0.5 of the normalized $R_{rs}667$. Diatoms were between 0.5 and 1 and between 0 and 0.5 of the normalized $R_{rs}488$ and $R_{rs}667$, respectively. Mixed species was also between 0.5 and 1 of the normalized $R_{rs}488$ and over 0.5 of the normalized $R_{rs}667$. Also, the non-bloom cluster was over 1 of the normalized $R_{rs}488$.

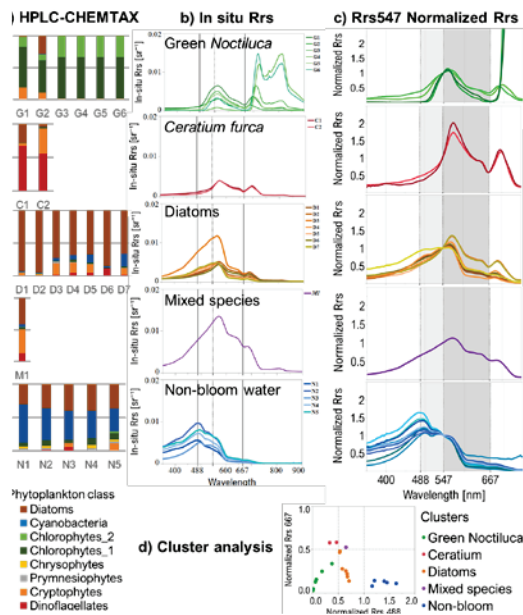


Figure 1 Results of each step of the HABs algorithm development.

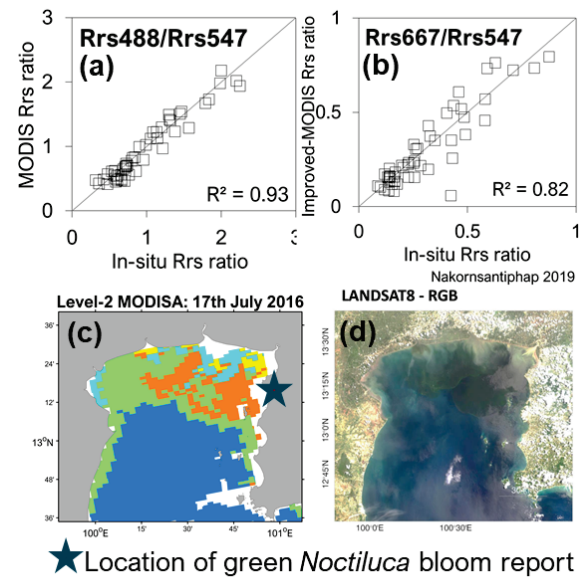


Figure 2 MODIS R_{rs} verifications (a-b) and the MODIS HABs image validated by comparing with the reported *Noctiluca* bloom (c) and the expected area of green *Noctiluca* bloom on Landsat 8 on July 17th, 2016 (d).

The incompatibility between the satellite and in situ R_{rs} appeared in the normalized $R_{rs}667$. The satellite R_{rs} data, thus, was improved the accuracy (Figure 2b). Then, the criteria of five clusters were applied to the satellite MODIS data (Figure 2d). The satellite image on July 17th, 2016 showed the broad area of green *Noctiluca* bloom in the east of UGoT. It was consistent with the dark greenish area on Landsat 8 RGB image (Fig. 2c and 2d) and with the report of green *Noctiluca* bloom at the eastern coast. This indicated that the algorithm could apply to investigate the location of green *Noctiluca* blooms using MODIS data in UGoT. The algorithm would be applied to other modern satellites such as VIIRS and GCOM-C in future works.

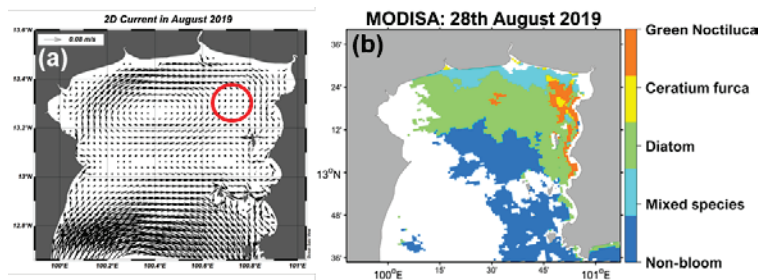


Figure 3 Simulated depth-averaged circulation comparing with the MODIS HABs classification in August 2019

The development of convergence in that area may also play a significant role in plankton cell accumulation. The blooming patchiness was expected to move to the east coast at the end of this month as shown in Figure 3b.

Periods of stay in ISEE: It has been canceled due to COVID19 outbreak.

List of publications: none

Simulated depth-averaged circulation in August 2019 (Figure 3a) is used to explain the occurrence of green *Noctiluca* bloom during the field observation on August 5-6, 2019. The accumulation of *Noctiluca* cell was found in the east of UGoT (red circle) because of river water advection following seasonal circulation.

Project: "Fluid-kinetic modelling of magnetic reconnection in solar flares and their impact on the heliosphere"

Investigators: from the University of Manchester - Dr Mykola Gordovskyy (PI), Prof Philippa K. Browning, Dr Gregory Vekstein, from ISEE - Prof Kanya Kusano and Dr Satoshi Inoue.

Background: Energetic particles carry a substantial part of the energy released in solar flares. A fraction of these particles escape from the solar corona into the interplanetary space, causing major disturbances in the heliosphere and near-Earth environment. The aim of this joint collaborative project is to investigate how solar energetic particles escape from the solar corona into interplanetary space. The key method is computational modelling using a framework combining MHD and test-particle approaches.

This project consists of two main elements. Firstly, we investigate how different topological configurations of magnetic field in the corona affect the properties of solar energetic particles and the fraction of energetic particles managing to escape from the solar corona. Secondly, we use the developed computational approach to model an actual flaring event.

The main added value of this collaboration is the combination of expertise in the solar coronal magnetic field reconstruction and MHD modelling of actual solar flares (Kusano et al. 2012 ApJ 760-31; Muhamad et al. 2017 ApJ 842-86; Inoue et al. 2018 Nat 9-174) with the expertise in MHD-test-particle (MHDTP) modelling (Gordovskyy et al. 2010 ApJ 720-1603; 2014 A&A 561-A72).

Timeline: 01/04/2019-31/03/2020

During the course of the project, MG, PKB and GV had a number of online meetings with our ISEE counterparts - Prof Kanya Kusano and Dr Satoshi Inoue. In June 2019 MG and GV visited ISEE for one week, and had a number of in depth discussions with ISEE colleagues, obtained MHD data for an individual flaring event and adapted it for test-particle simulations. (Another visit, originally planned for March 2020, has been postponed due the coronavirus travel restrictions).

The main outcomes of the project:

- We have considered proton and electron acceleration in three different generic models involving unstable twisted magnetic fluxtubes in the solar corona. In two of the models - one with open and one with closed ambient magnetic field - the twisted fluxtube did not erupt. In the third model, the twisted fluxtube did erupt. It was found that even in the configuration with the erupting fluxtube and ambient magnetic field "open" into the interplanetary space, the number of particles escaping into the interplanetary space was below 10-15%. This result is consistent with observational estimations, showing that the number of energetic electrons escaping into the interplanetary space after solar flares is much lower than a number of energetic electrons precipitating in the corona (Krucker et al. 2007 ApJ 663-L109). Our provisional interpretation for this effect is that the field strength in the "closed" magnetic field is, on average, higher than in "open" magnetic field and, hence, "closed" magnetic field is more efficient in capturing energetic particles. These results will be prepared for publication in the *Astronomy & Astrophysics* later this year.
- We have constructed an MHDTP model of an actual X-class flare which occurred on 06/09/2017. Using this model, we have investigated spatial and temporal characteristics of the acceleration region, and evaluated the properties of energetic particles (their spatial distribution, temporal evolution and energy spectra). Furthermore, using the trajectories of energetic electrons, we have calculated locations and relative intensities of the photospheric

hard X-ray (HXR) bremsstrahlung sources. Based on these results, we have prepared a manuscript, which is expected to be submitted to the Astrophysical Journal by the end of May 2020. Furthermore, these results have been reported during the Solar Orbiter meeting (University of St Andrews, January 2020).

- We have identified two other solar flares which will be investigated using MHDTP modelling during this year – X-class flares which occurred on 13/02/2011 and 15/02/2011. We have obtained and analysed HXR observations of these flares by RHESSI. The next step will be to calculate particle distributions for these events and predict the locations and intensities of hard X-ray sources. By comparing the synthetic hard X-ray maps with those observed by RHESSI, we will be able to test the reliability of the MHD-test-particle approach in modelling individual flaring events.

This result will provide an important basis for future work. When our MHDTP computational framework is adapted for modelling individual flaring events, it will be very useful for interpreting remote observations of non-thermal emission (HXR, microwave, low-frequency radio) from individual solar flares, as well as their in-situ observations in the inner heliosphere by two new instruments – Parker Solar Probe and Solar Orbiter missions.

Investigation of the relationship between nighttime electrified medium scale traveling ionospheric disturbances and middle latitude spread F

Viswanathan Lakshmi Narayanan
(UiT The Arctic University of Norway)

Purpose

It is currently believed that the spread F in middle latitudes are caused by nighttime electrified medium scale traveling ionospheric disturbances (EMSTIDs). However, it is noted in the earlier works that spread F does not occur whenever EMSTIDs occur. We proposed to investigate the relationship between nighttime EMSTIDs and middle latitude spread F in detail. Meanwhile, the affiliation of the Principal Investigator has changed and as a consequence, additional research is done on the mesospheric dynamics and its role in altering sodium densities. This latter work has led to interesting preliminary results that are submitted for the forthcoming EGU General Assembly meeting as given in the publications section.

Methods

We approach the problem of relationship between EMSTIDs and spread F with the help of GPS TEC data and ionosonde measurements over Japan with plans to utilize airglow imaging observations at a later stage. We selected the summer months of recent solar maximum year of 2014. This is done to have a few days without EMSTIDs so that we can also identify whether spread F forms when there is no EMSTIDs. If we select solar minimum year, it is likely that spread F and EMSTIDs will form every day making the discrimination difficult. However, being a weak solar maximum year, almost every night has EMSTID signature in summer 2014. We studied the GPS TEC data around the ionosonde measurement sites of Wakkanai (45.16°N, 141.75°E geographic; 38.46°N quasi dipole), Kokubunji (35.71°N, 139.49°E geographic; 28.72°N quasi dipole), Yamagawa 31.20°N, 130.62°E geographic; 24.54°N quasi dipole) and Okinawa (26.68°N, 128.15°E geographic; 20.01°N quasi dipole) during May to August 2014. The standard deviation of detrended TEC and average of ROTI indices are made for a region of 300 square kilometer centered at the ionosonde sites. The existence of spread F and sporadic E are noticed from respective ionosonde measurements. An enhancement in the standard deviation of detrended TEC (dTEC) indicates existence of EMSTIDs.

Results

Earlier works have shown that spread F occurs only for part of the time when there are EMSTIDs. Our results confirm the earlier findings in that the observed spread F events almost always occur when there is some presence of EMSTIDs. However, on rare instances spread F

occurs without corresponding existence of EMSTIDs. Couple of examples are shown in the Figure below. Among the variety of parameters checked, the figure shows the standard deviation of dTEC as indication for existence of EMSTIDs along with the blue stars representing spread F. Note that there is spread F without noticeable EMSTID activity over Wakkanai on 3 May (left image) and Yamagawa on 24 July 2014 (right image). The other stations have spread F with reasonable EMSTIDs. Another general trend we noticed is that the amplitude of the EMSTID perturbations during existence of spread F is relatively higher when the latitude of the observation location is lower. This is seen often with higher amplitude EMSTIDs over Yamagawa and Kokubunji compared to those over Wakkanai. We identify that high spatio-temporal resolution data is required from middle latitude E and F region ionosphere to comprehensively understand the processes linking the EMSTIDs and spread F formation.

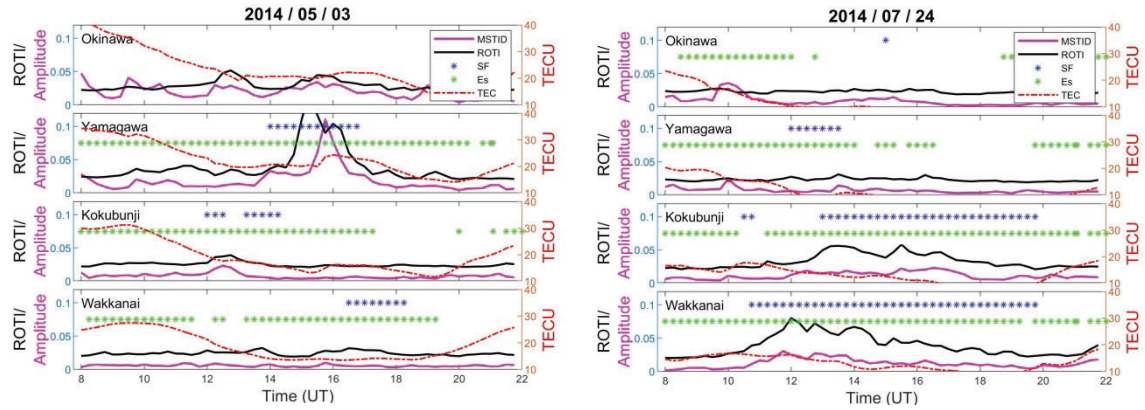


Figure 1. TEC parameters, spread F and sporadic E occurrences on 3 May and 24 July 2014

Period of stay in ISEE

Viswanathan Lakshmi Narayanan stayed in ISEE, Nagoya University between 10 December 2019 and 15 January 2020 to carry out the abovementioned works. Part of the work is completed before the visit and remaining is being continued till now.

List of publications

V. L. Narayanan, S. Nozawa, I. Mann, S. Oyama, K. Shiokawa, Y. Otsuka, N. Saito, Mesospheric fronts in airglow images and the variation of the bottomside sodium layer densities measured by a sodium lidar at Tromsø, Norway, submitted to the EGU General Assembly 2020.

The NoRH/RHESSI flare catalogue: statistical paper and planning for the future

Säm Krucker, FHNW & UC Berkeley

Solar flares give us a unique opportunity to make spatially resolved observations to study magnetic energy release and particle acceleration in space plasmas. The most direct diagnostics of electron acceleration are provided through radio and hard X-ray observations where we observe synchrotron emissions in the GHz range and non-thermal bremsstrahlung emissions above typically 10 keV. Observations at these two different wavelength ranges are highly complementary as synchrotron emission heavily depends on the magnetic field along which the electrons spiral, while bremsstrahlung is weighted by the ambient density where the electrons suffer collisions. The two leading solar dedicated observatories of the past decades are the Nobeyama Radioheliograph (NoRH) and the Reuven Ramaty High Energy Solar Spectroscopic Imager (RHESSI). Both observatories apply indirect imaging techniques heavily relying on sophisticated imaging reconstruction algorithms to achieve the best possible results.

During my research stay at University of Nagoya as visiting professor in May through July 2018, I compiled a list of jointly observed large flares establishing the NoRH/RHESSI large flare catalogue. The catalogue contains statistical results on peak flux, time evolution, and imaging. With the RHESSI mission now being decommissioned, this set of events is the final catalogue and contains the best available data on jointly observed flares in microwaves and hard X-rays for years to come.

During my research stay from October 21 through November 21, 2019, we completed the following tasks:

- 1) We wrote a paper containing the main statistical results obtained so far. The papers main finding is the correlation plot between radio and hard X-ray peak flux that extends over 4 orders of magnitude, corroborating that a single accelerator produces both, the microwave and hard X-ray emitting electrons (see Figure 1). By restricting the correlation to flares with the same source geometry, we showed that the correlation further improves. We got positive feedback from the referee, and the paper will be accepted by end of March 2020.
- 2) We analyzed the strong event within our sample (Feb 25, 2014) with a peak flux above 20k SFU for which the standard imaging approach fails with a new approach. The event is included in the statistical paper mentioned above.
- 3) We made plans for future collaborative effort between UCB, FHNW, and ISEE to further

exploit the unique set of events selected in the NoRH/RHESSI catalogue. This includes the analysis of common events seen with the SUZAKU/WAM instruments, and the search for the smallest non-thermal flares with peak fluxes at 17 GHz below 1 sfu seen by NoRH.

List of publication:

- Krucker, Masuda, & White, 2020, *Astrophysical Journal*, under review

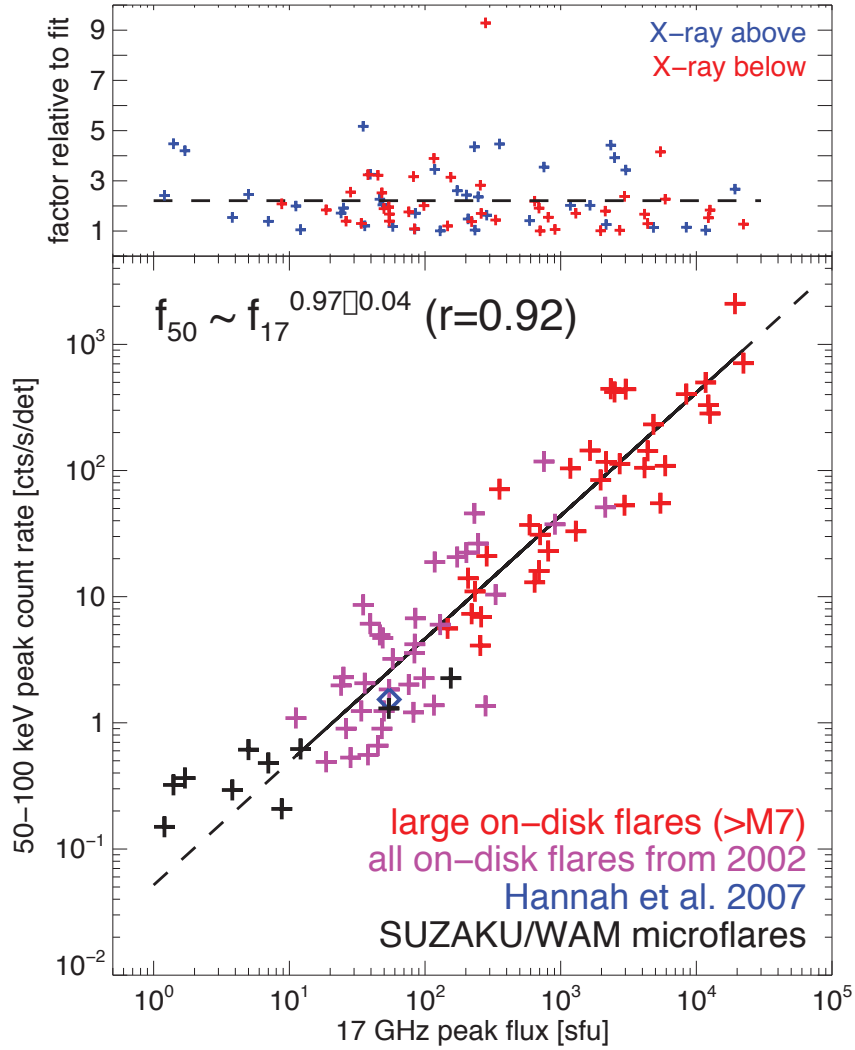


Figure 1: Correlation plot between the 17 GHz peak flux and the 50-100 keV peak count rate. Top panel show the factor of deviation from the fit. Note the linear correlation over more than 4 orders of magnitude with an averaged scatter of about a factor of 2.

Energetics of Arctic Stratospheric and Mesospheric Coupling Due to Small-scale Gravity Waves

Kim Nielsen (Utah Valley University)

Comment: The COVID-19 pandemic overlapped the period of this project and put some restrictions on the progress of the project as well as presenting the work at conferences. We will pursue the remaining part of the project and publications as soon as the COVID-19 restrictions allow. Specifically, this limited the effort involving the airglow image analysis.

Background

Small-scale gravity waves play a major role in energy transfer throughout the atmosphere and near-space environment, and therefore are essential to include on both weather and climate model studies. However, due to their small structure, they are difficult to implement into these models. Instead, they are often parameterized through an ensemble effect of energy transfer, with the assumption that the energy transported from the source is deposited at the wave breaking level. This assumption is questionable as we know from observations that energy may be dissipated at various altitude levels as the waves propagate through the atmospheric layers. This intermittent energy and momentum transport are not well documented in the literature.

Objectives

1. Investigate the energetics of gravity waves in the Arctic upper mesosphere and lower thermosphere (MLT) utilizing the derived temperature and winds from the Na lidar situated at Tromsø, Norway.
2. Extend the data product capability of the Na lidar system to include its Rayleigh signal in the stratosphere for exploration of stratospheric gravity wave analyses.
3. Combine coincident lidar and airglow imaging to explore the vertical and horizontal characteristics of energy/momentum transfer in the MLT region by individual gravity waves.

Methodology

The Na lidar data used in this study to date included profiles obtained over the period January 2013 – February 2019, and was categorized into three quality tags: low, medium, high, based on the duration of nightly measurements (high: 6+ hours and no intermittent data gaps). Extracting wave information from lidar signals have been done in numerous studies utilizing a wide range of processing options. According to [Ehard et al., \(2015\)](#) the recommended method to extract gravity wave information from lidar profiles is to utilize spectral filtering method with a Butterworth filter.

To prepare the lidar data for proper signal processing, the data was mirrored to resemble a periodic signal prior spectral analysis. To assess the energy content in the wave field, a Butterworth filter was applied to extract the wave components of interest, the nightly background temperature and natural frequency profiles were determined, and the gravity wave potential energy density was calculated as a function of altitude. The wavelet/S-transform analysis was applied to the data to assess the variability of the wave field as a function of period and altitude.

Results

Our objectives are restricted to wave fields exhibiting periods on the scale of a few hours and down to a few minutes as well as limited in vertical wavelength by the altitude range covered by the lidar but

also the minimum vertical resolution of an airglow imaging systems. One can filter in time or spatial domain (or in principle in both). The recommendation by [Ehard et al., \(2015\)](#) is spatial filtering, which we also confirmed in our analysis. Following the methodology outlined above, Figure 1 shows a case study profile of the potential energy density as a function of altitude.

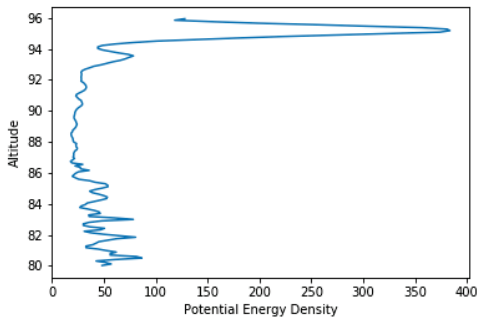


Figure 1: Example potential energy density profile for a wave field observed on January 9th, 2014.

The accumulative potential energy density typically observed in the Na lidar data varies between ~ 600 - 900 J/kg, which is within the range reported by other studies. We observe from the figure that the potential energy density exhibits variability across the altitude range, and it is this variability we are seeking to quantify. Typically, we see a decrease most likely due to wave breaking and dissipation in the altitude range 85-90 km with a subsequent increase suggesting 1) that the wave field did not experience wave breaking but rather underwent intermittent energy transfer, or 2) the wave field experienced wave breaking and secondary waves formed which propagated the energy

upward. Further analysis is needed to evaluate these scenarios.

Figure 2 shows an example result of the wavelet analysis revealing the spectral characteristics of the wave field (power spectral density as a function of wavelength and altitude). This result suggest the majority of the wave power is contained in the gravity waves with small vertical wavelength (2-4 km), and there is suggestive evidence of wave generation of a 4 km vertical wavelength signal near 94 km, suggesting possibility (2) above (secondary wave generation) plays a role in the observed energy transfer.

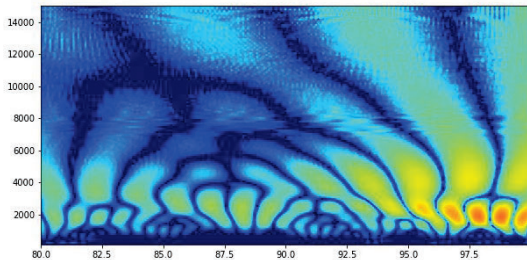


Figure 2: Wavelet power spectral density as a function of altitude (horizontal axis) and vertical wavelength (vertical axis).

In addition to Na resonance scattering signals, the Na lidar observations have been accumulating Rayleigh scattering signals in the major atmospheric particles, such as N_2 and O_2 , from the stratosphere to the mesosphere. The Rayleigh scattering signals can be used for getting temperature data in the height range. Thus, such temperature data would provide important information on the coupling of upward propagating atmospheric waves into upper mesosphere and lower thermosphere. During the current project, we have

developed a software to derive temperature data from the Rayleigh scattering signals. After the brief validation on the calculated temperature data, we have processed data covering the period between 2011 to 2019. The obtained long-term temperature data would be expected to advance our understanding of the vertical coupling in the polar atmosphere thorough the atmospheric waves.

Periods of Stay in ISEE January 6 – 26, 2020

List of Publications None

Tomographic study of galactic cosmic anisotropy in near-Earth space by Multi-directional cosmic ray observatory

P. K. Mahanty (Tata Institute of Fundamental Research, India)

The propagation of galactic cosmic rays (GCRs) through the heliosphere and especially their interaction with the interplanetary magnetic field in the inner heliosphere impacts the space weather. The significance of characterizing the GCR propagation is self-evident, since it can provide a practical capability of forecasting effects of space weather that have implications for the successful operation of technological infrastructure on Earth and in space. There is an active ongoing participation of several Japanese scientists in the GRAPES-3 experiment located in Ooty, India which contains the world's largest (560 m²) muon telescope that detects GeV muons produced by the interaction of cosmic rays in the atmosphere. Its observations enable to monitor the electromagnetic environment of the near Earth space through detection of tiny changes in the cosmic ray intensity variation even in a short timescale of minutes. The GRAPES-3 has recorded an uninterrupted 20-year data base of muon intensity with the highest sensitivity covering solar cycles 23 and 24. The space weather studies through the diffusion of high-energy GCRs are extremely valuable since they serve as a probe of relatively larger scale structures in the interplanetary space and provide information complementary to that obtained from the low-energy measurements using space-based probes and neutron monitors. The ISEE international joint research program had supported the visit of two scientists from TIFR, India to Nagoya during October 2016. During the visit, the work on the measurement of radial diffusion coefficient of GCRs in the heliosphere using the GRAPES-3 muon data from the period 2000 to 2005 obtained from two independent methods (i) the correlated variations of solar wind velocity and GCR flux (Kojima et al., Physical Review D 91, 121303(R) (2015)) and (ii) the GCR radial density gradient from Swinson flow (Kojima et al. Astroparticle physics 62 (2015) 21)) were extensively discussed. It was found that the radial diffusion coefficient from the two independent methods yielded a similar value of $\sim 10^{19} \text{ m}^2 \text{ s}^{-1}$ at 1 AU, characterizing the diffusion of GCRs at 77 GV. From this value of radial diffusion coefficient, the mean free path length for parallel diffusion was estimated to be 1.2 AU at 77 GV. These results led to a publication in a peer reviewed journal (Kojima et al., Phys. Rev. D 98 (2018)). This work has been further extended to examine the dependence of these parameters on the solar activity based on the sunspot number. With the support of the ISEE international joint research program for 2019-2020, two team members from TIFR, Mumbai including the PI of this project and Prof.

S.K. Gupta visited Nagoya during the period of 16 February to 7 March 2020 to discuss the analysis and preparation of a paper on these results. A brief summary of the activities performed during the visit is described below.

Profs. H. Kojima, S. Shibata, A. Oshima, Y. Muraki, S. Kawakami, Y. Hayashi, S.K. Gupta, and Dr. P.K. Mohanty met at the Chubu University and had very extensive discussion over the work carried out by Prof. H. Kojima on the relation between the cosmic ray density gradient and the sunspot number. Similar analysis as performed for the two papers mentioned above were extended to 17 years of GRAPES-3 data for the period from 2000 to 2016. The cosmic ray intensity variation with solar wind velocity was found to have a strong anti-correlation with the sunspot number. A strong linear correlation between GCR density gradient and sunspot number was observed. Several new ideas emerged during the discussion. Writing of a manuscript on this work to publish it in a peer reviewed journal was started during the visit. The finalization of the paper was expected during the visit of Profs. H. Kojima, S. Shibata and S. Kawakami to TIFR, Mumbai later in March 2020 which unfortunately had to be cancelled due to the Covid-19 outbreak.

A seminar was delivered by Prof. S.K. Gupta at the Nagoya University on 25 March 2020 with the title “Study of Cosmic Rays by GRAPES-3: A powerful messenger in the universe”. The seminar discussed about the result of the transient weakening of Earth’s magnetic shield by the GRAPES-3 muon telescope and its potential for accurate prediction of arrival of solar storms. The measurement of the record break potential during thunderstorm using the GRAPES-3 muon data was also highlighted. It was attended by several faculty members of the ISEE. Although many of them do not work in cosmic rays, however the topic was a common interest to several members and led to fruitful discussions.

Members including Profs. H. Kojima, A. Oshima, S. Kawakami, Y. Hayashi, S.K. Gupta, Y. Nakamura and Drs. P.K. Mohanty, K. Yamazaki and T. Nonaka visited the Akeno Observatory in the Yamanashi prefecture during 1-3 March 2020. Prof. K Tanaka from Hiroshima joined the discussion through Skype. It was a rare opportunity to have a meeting of so many members at one place. A very fruitful discussion occurred to analyse the GRAPES-3 muon data as well as the Akeno muon telescope data. A discussion occurred to upgrade the Akeno muon telescope which operates 3 modules similar to GRAPES-3.

In summary, the visit was very productive though it had to be shortened by a week due to the pandemic. The PI and the team members are thankful to the support of the ISEE.

Imaging meter-scale density irregularities associated with midlatitude TIDs

Hiroatsu Sato (DLR)

Purpose

The objective of this ISEE International Joint Research Program is to understand small scale density structures down to meter scale associated with midlatitude Traveling Ionospheric Disturbances (TIDs) by using L-band spaceborne Synthetic Aperture Radar (SAR) and GNSS observations. TIDs are wave-like plasma density perturbations propagating in the ionosphere. Night time TIDs, often observed at middle latitude, can have typical scale sizes of several hundreds of kilometers and wavelength of a few hundreds of kilometers. It is reported that the 3-m scale field-aligned irregularities in F region simultaneously with night time TIDs. We aimed to experimentally better understand the small scale structure of TID.

Method

The propagation of TIDs can be efficiently monitored by two-dimensional total electron content (TEC) maps from ground GPS/GNSS receiver network. In addition, low-frequency synthetic aperture radar (SAR) systems have been suggested to achieve the mapping of small-scale ionospheric TEC distributions at a finer resolution than do GPS/GNSS measurements. Therefore we have used simultaneous observation of MSTID over Japan by using data from GEONET GNSS data and ALOS/ALOS-2 SAR systems.

Results

When an event of night time MSTID over Japan was observed by GEONET TEC on 2019-08-20, ALOS 2 acquired ground SAR images from Chiba to Niigata area. The perturbation component of GNSS TEC modulation is approximately 0.5 TECU. From the quad pol SAR data, we have estimated Faraday rotation of SAR signals originated from ionospheric propagation and converted it to SAR-TEC map over approximately 50x400 km swath. Our preliminary analysis shows that 0.5 TEC modulations are also found in SAR TEC when mapped to F region altitudes near TID wave front. We will further investigate this observation with intention to achieve km scale TEC mapping as a continuation of the research project and we aim at a scientific publication this year.. Figure 1 shows GEONET TEC and SAR observation of the MSTID event.

20190820 14:30 UT

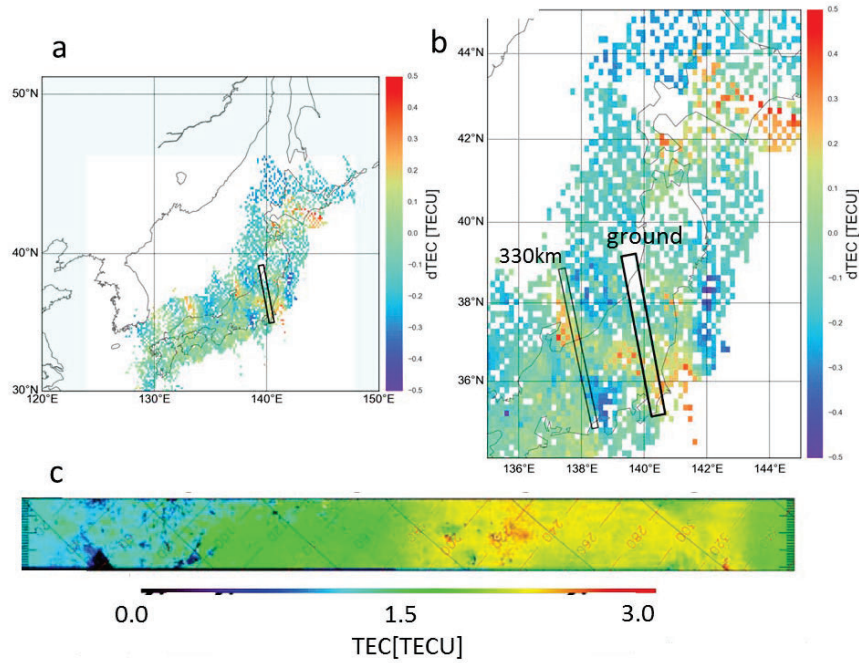


Figure 1 (a) GENET TEC observation of MSITD on 2019-08-20. (b) TEC perturbation near SAR observation frame at ground and projection at 330 km altitude. (c) Estimated SAR TEC.

Research stay at ISEE

I have stayed at ISEE between October-November 2019 and January – March 2020. During these stays, I have participated SGPSS in Kumamoto and PSTEPS symposium in Nagoya. I was also given an opportunity to hold a seminar for ISEE Division for Ionospheric and Magnetospheric Research where I enjoyed fruitful discussion with the lab members.